Chapter 8-3-3
Acid altered terrains: Formation, hazards and related uses

Hiroshi Shinohara (Geological Survey of Japan, AIST) shinohara-h@aist.go.jp
Pierre Delmelle (UCLouvain) pierre.delmelle@uclouvain.be
Carol Finn (U.S. Geological Survey) cfinn@usgs.gov
Michael J. Heap (Université de Strasbourg, CNRS, Institut Terre et Environnement de Strasbourg, UMR7063) heap@unistra.fr
Jeffrey W. Hedenquist (University of Ottawa) jhedenquist@gmail.com
Dmitri Rouwet (Istituto Nazionale di Geofisica e Vulcanologia, Sezione di Bologna, Italy) dmitri.rouwet@ingv.it
Bettina Scheu (Ludwig-Maximilians-Universität München) b.scheu@lmu.de
Vincent Van Hinsberg (McGill University) vincent.vanhinsberg@mcgill.ca

(Sections in this chapter are citated in text by the section numbers, e.g., §1).

SDGs 1, 2, 3, 6, 7, 8, 9, 11 and 15.

Abstract (for Web site)

Hydrothermal activity and related alteration is common in volcanic environments. Acidic condensates (pH~1–2) of volcanic gases react with rocks and create alteration minerals along chemical and thermal gradients in the hydrothermal system on flanks of many active volcanoes. Such alteration ranges from acid leaching outward to clay formation at less acidic conditions, as the rock neutralizes the acids. Geological studies of outcrops and geophysical imaging reveal the distribution of alteration minerals below the surface. Alteration affects the mechanical properties of volcanic rocks, which may contribute to slope failures and influence fluid flow pathways and the location of hydrothermal eruptions. Drainage of the acid solutions, commonly with abundant toxic components, may lead to environmental contaminations. After formation of alteration by the acidic condensates, ascent of subsequent liquid may precipitate Au and Ag plus Hg, Cu, Pb and Zn, forming epithermal metal deposits within ~1 km of the surface, the major ore type hosted by the products of acidic alteration.

Keywords
Volcanic gas, Hydrothermal fluids, Vapor-liquid separation, water-rock interaction, Clay formation, Crater lake, Hydrothermal eruption, Epithermal metal deposit, Acid drainage, Alteration-induced hazard

Glossary

Hydrothermally altered rock: fluid-rock interaction with chemical changes of primary to alteration minerals, forming hydroxyl, carbonate ± sulfate and aluminosilicate minerals as well as quartz or amorphous silica.

Hydrothermal eruption: Sharp depressurization of hydrothermal fluid (H_2O, CO_2, etc.), due to e.g, dike intrusion or seismicity, causes the liquid to boil. The resulting vapor expansion contributes to fracturing and eruption. The vapor-static eruption column consists of muddy vapor and lithic clasts, typically altered. If juvenile magma is included, the eruption is magmatic hydrothermal.

Epithermal ore deposit: Formed within ~1-1.5 km of the surface at temperatures <300 ºC; many such deposits have a transition to the porphyry ore environment (epi is Greek for over or above). Metals (Au, Ag, Hg, As, Sb ± Cu, Pb, Zn) precipitate in fractures (veins) or pore spaces (disseminated) from liquids of a volcanic hydrothermal system.

Phreatic eruption: Also called a phreatic explosion, occurs when magma heats ground water or surface water (lake or ocean).

Volcanic hydrothermal fluids: H_2O-dominant fluid (with CO_2, S species, NaCl, and other components) exsolved from a magma during shallow (<3–4 km) crystallization beneath a volcano, typically mixed with meteoric ground water at shallow depth.

1. Introduction

This chapter focuses on the shallow features (<1 km depth) of volcanic-related hydrothermal systems that are acid altered, including associated resources, hazards and environmental effects. Hydrothermal alteration is a common feature proximal to volcanic vents. Acidic condensates (as low as pH~1) of volcanic gases react with rocks and create alteration minerals along chemical and thermal gradients in the volcanic hydrothermal system. Alteration changes the physical and mechanical properties of volcanic rocks, promoting slope failure, and affects fluid flow pathways and location of hydrothermal eruptions. Drainage of acid waters, commonly rich in toxic components, may create environmental and health hazards. After the formation of acid alteration, the ascent of subsequent liquid may deposit Au and Ag plus Hg, Cu, Pb, Zn and other critical elements, forming epithermal metal deposits within ~1 km of surface, the major ore type hosted by the products of acid alteration.

2. Volcanic hydrothermal systems

Active and dormant volcanoes commonly host volcanic hydrothermal systems near their summits and flanks ([1], Fig. 1), with variable magmatic contributions (heat plus chemical components). Where reactive hydrothermal solutions – condensates of magmatic vapor – interact with fresh volcanic rock during ascent, the alteration may weaken the mechanical properties of rocks (§4.2), leading to failure and landslides (§6.1). The alteration minerals form halos around fractures that provide conduits for subsequent hot liquid to rise; metals may also precipitate from this liquid to form shallow (<1 km depth) ore deposits.

Magma bodies that intrude the volcanic edifice of eruption products consist of stocks and dikes at 2–4+ km depth below surface (Fig. 1). The intrusions commonly have large phenocrysts and fine groundmass, a texture referred to as porphyritic [2]. As crystallization proceeds, an aqueous fluid (~5–10 wt% NaCl equiv.) saturates and exsolves from the melt; this ascending solution is referred to as *hypogene* in origin. Ascent to ~2 km depth results in pressure decrease and separation to hypersaline liquid (40–60 wt% NaCl equiv.) and a low-salinity vapor (Fig. 1, stage 1). The hypersaline liquid creates biotite–K-feldspar alteration at >500 ºC during this initial stage. The low-density vapor that separates from the early hypersaline phase (recorded in fluid inclusions of ore deposits; Fig. 1) rises to the surface to discharge from fumaroles (Fig. 1, stage 1) at temperatures as high as 900+ ºC (Fig. 2a). This magmatic vapor is dominantly H_2O, but also contains acidic gases such as CO_2, SO_2, H_2S, and HCl. Part of the vapor condenses into groundwater of meteoric (rainwater) origin at several 100s m depth, forming highly reactive acidic solutions of H_2SO_4 (reaction 1) and HCl (reaction 2), which alter the rock.

$$4\ SO_2\ (g) + 4\ H_2O\ (l) \Leftrightarrow H_2S\ (aq) + 3\ SO_4^{2-}(aq) + 6\ H^+(aq) \quad (1$$

$$HCl(g) \Leftrightarrow Cl^-(aq) + H^+(aq) \quad (2$$

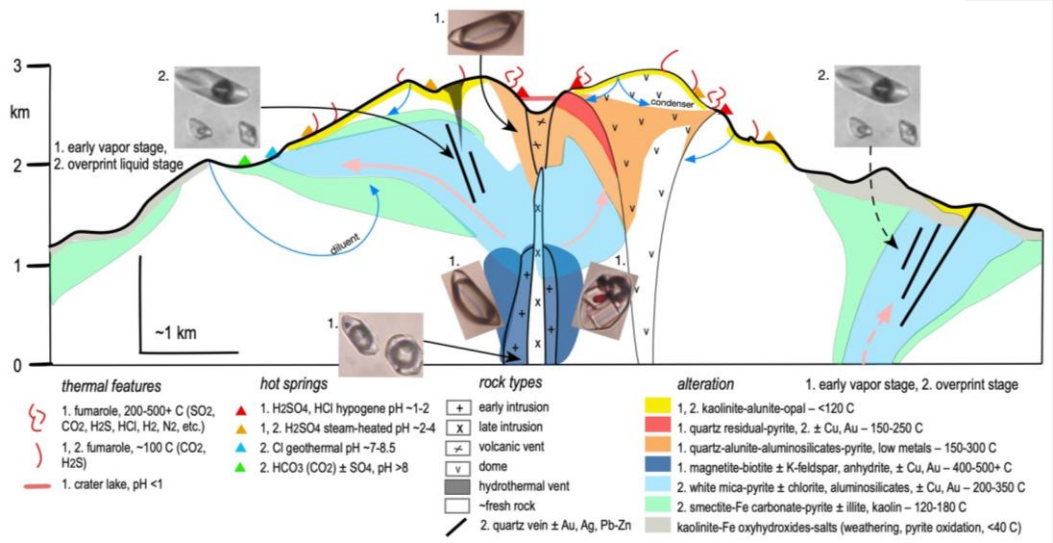

Fig. 1 Volcanic massif with multiple intrusive centers and related hydrothermal activity, some now extinct (partly eroded with grey near-surface weathering, left and right margins; flow paths shown). Ascent and pressure decrease of the aqueous liquid exsolved from the intrusion (deepest fluid inclusion photograph; 20-40 μm width) separates to dense hypersaline liquid (stage-1; dark blue) and high-temperature H_2O-rich vapor (*hypogene*, §2); as recorded by stage-1 fluid inclusions (photographs next to intrusion). The low-density vapor phase (H_2O, CO_2, SO_2, HCl, H_2S, etc.) ascends and discharges as high-temperature fumaroles (Fig. 2a), or partially condenses into groundwater (blue arrows) to form hyperacidic (pH~1) solutions (§2) that leach rock to leave residual silica, with alteration halos of quartz-alunite and aluminosilicates (red, orange). Accumulation of condensate in crater lakes (Fig. 2b) becomes hyperacidic (pH<1) due to evaporation. Condensation of ~100°C fumaroles causes H_2S oxidation to sulfate (reaction 3; yellow), creating *steam-heated* horizons of pH~2-4 solutions and kaolinite blankets. Later stage-2 liquid (light blue, <5-10 wt% NaCl) has a component of lateral flow (pink arrow) due to hydraulic gradients; near-neutral pH chloride hot springs discharge on lower flanks after dilution by deeply circulated meteoric water (blue arrow), precipitating silica sinter (Fig. 2c). CO_2-rich steam-heated condensates (reaction 4; green) discharge as bicarbonate (HCO_3)-rich springs. Metals (Au-Ag, Cu, Pb-Zn) may precipitate during ascent of stage 2 liquid due to cooling caused by boiling or groundwater mixing at <1 km depth, in veins or brecciated residual quartz (pink arrows, dashed where extinct). Erosion exposes altered rock with pyrite, which oxidizes to form acidic *supergene* solutions (grey). [3] and references therein.

A large rate of magmatic fluid release can be achieved by the rapid cooling of the magma body, caused by the intrusion into a cool crust; convection in the magma body causes rapid heat and fluid loss. The magmatic fluid release rate decreases with time, causing the maximum temperature of the hydrothermal liquid at ~2 km depth to be ~350 °C, meaning that it does not separate (Fig. 1, stage-2 fluid inclusions) in the later stage. This low salinity (i.e., ~5−10 wt%

NaCl equiv.) liquid forms white mica and chlorite alteration, with dilution by deeply circulating meteoric water prior to discharge as neutral pH hot springs.

Interaction of SO_2 and HCl with wallrock results in these reactive gases being consumed (reduced and neutralized, respectively), and vapors on the margins becoming CO_2 and H_2S rich ([4] and references therein). Condensation of this CO_2- and H_2S-rich vapor at ~100-150 ºC, long referred to as *steam-heated* solutions, forms two other sources of acidity. Where the vapor condenses above the groundwater table, in the unsaturated vadose zone (Fig. 1), the H_2S is oxidized by atmospheric O_2 to H_2SO_4 (reaction 3); the pH ~2–4 solutions form blankets of steam-heated kaolinite alteration above the water table (Fig. 1), with CO_2 bubbling through the mud pools. By contrast, where this vapor condenses below the ground water table, the CO_2 goes into solution (as H_2CO_3, reaction 4); the pH ~4–5 steam-heated solution forms clay-rich alteration on the margin of the system (Fig. 1).

$$H_2S(g) + 2\ O_2(aq) \Rightarrow SO_4^{2-}(aq) + 2\ H^+(aq) \quad (3$$

$$H_2O(l) + CO_2(g) \Leftrightarrow HCO_3^-(aq) + H^+(aq) \quad (4$$

A fourth source of acidity is generated where pyrite (FeS_2) – formed during alteration and exposed by erosion – is weathered and oxidized (reaction 5, mediated by bacteria such as *A. ferrooxidans*), to create acidic solutions of H_2SO_4 with pH as low as 0. Such weathering alteration is referred to as *supergene*, and may continue long after hydrothermal activity ends.

$$FeS_2(s) + 3.5\ O_2(aq) + H_2O(l) \Leftrightarrow Fe^{2+}(aq) + 2\ SO_4^{2-}(aq) + 2\ H^+(aq) \quad (5$$

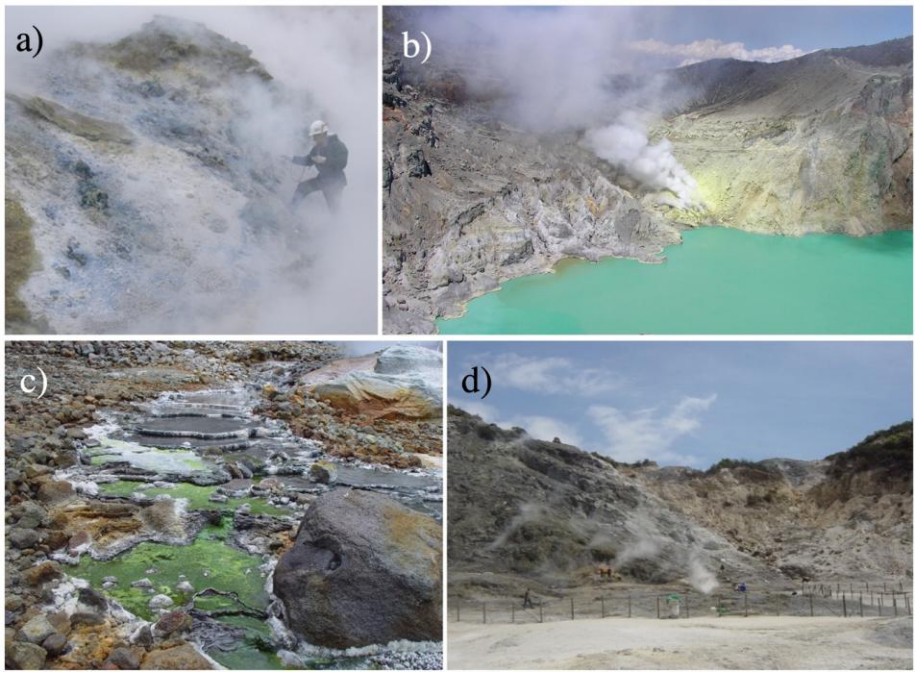

Fig. 2 Photos of surface manifestations. a) High-temperature fumarole (861°C) at Satsuma-Iwojima (Japan)(HS). b) Acidic crater lake of Ijen volcano (Indonesia)(VV). Elemental sulfur (yellow) around fumaroles forms from H_2S and SO_2 in volcanic vapors (reaction 6, 7). c) Hot springs with amorphous silica sinter rim, El Chichón (Chiapas, Mexico)(DR). Cl-rich, near-neutral pH boiling spring originates from the Soap Pool Geyser (upper right) and discharges over sinter terraces and drains into a pH 2.5 crater lake. d) Solfatara (Italy) of CO_2-rich fumaroles, ≤160 °C, with strong alteration inside crater (HS).

3. Distribution of the fluids and alteration

3.1. Surface manifestations

A variety of surface features of volcanic hydrothermal systems occur on the summit and flanks of volcanoes, including fumaroles with various temperatures, hot spring liquids of acidic (pH~1) to alkaline (pH>8) composition, and acidic crater lakes (pH≥0), all with associated alteration. Distribution of the surface manifestations is largely controlled by the degree of a magmatic vapor condensed into meteoric water or seawater. Direct ascent of a high-temperature magmatic vapor, such as at open-conduit degassing volcanoes, does not create significant alteration at and near the surface despite the large gas flux, due to limited interaction with meteoric water in aquifers. Where shallow aquifers are saturated with meteoric water, the magmatic vapor condenses to form acid solutions that discharge as acidic hot springs (Fig. 1) with a pH as low as ~1 (reactions 1 and 2). Heating or cooling

of the volcanic hydrothermal system, related to changes in volcanic activity, results in evaporation or condensation, respectively, and changes in fumarole compositions [4].

Crater lakes may form in depressions caused by volcanic or hydrothermal eruptions, accumulating acidic solutions with pH values <1 due to evaporative concentration of the acids (Fig. 2b). The hyperacidic (pH<1) crater lakes (such as Poás, Costa Rica, and Kawah Ijen, Indonesia; Fig. 2b) have green to blue colors due to high concentrations of Al, Fe, sulfate (up to % values) and chlorides in solution, and colloidal silica and native sulfur in suspension. The cations in the acidic solution are isochemically dissolved from the host rock, except for silica, leading to large areas of alteration. The alteration is zoned from proximal residual amorphous silica (recrystallized to silica polymorphs, including quartz), with outward halos of alunite and aluminosilicate minerals (kaolinite, dickite) plus smectite to illite clays, mixed with a variety of efflorescent salts (Fig. 1).

Where low-salinity hydrothermal liquid of near-neutral pH ascends (stage 2), it discharges in topographic lows and on volcanic flanks as hot springs, up to several km from the volcanic summit (Fig. 1), typically depositing amophous silica in layers, called sinter (Fig. 2c). Fumarolic vapor rich in CO_2 and H_2S, separated from a boiling liquid, condenses above the groundwater table in the unsaturated vadose zone (Fig. 1). These low-temperature fumaroles (reaction 3) form large areas of steam-heated kaolinite alteration (e.g., Solfatara, Campi Flegrei, Italy; Fig. 2d). Hydrogen sulfide in the vapor, and SO_2 if present, form elemental sulfur upon cooling (reaction 6) that deposits around low-temperature fumaroles (§5.2; Figs. 2b and 8e).

$$SO_2(g) + 2H_2S(g) = 3S_e(s) + 2H_2O(g) \quad (6$$

Where deeper CO_2-rich steam-heated solutions reach the surface, degassed bicarbonate springs form carbonate terraces of travertine.

3.2. Subsurface: Geological model

A volcanic hydrothermal system can be several km^2 in size, even though the surface features may be more restricted in area, e.g., along faults, and extend to 2-3+ km depth, overlapping with the crystallized intrusive center of the system [2]. The aqueous solution that is most reactive – creating the strongest alteration – forms due to vapor with acidic volatiles (reactions 1 and 2) condensing into groundwater. By contrast, on the margins of the volcanic hydrothermal system, the acidity is neutralized by reaction with feldspars and other components in fresh rock, as well as by increasing dilution by meteoric water. The near-neutral pH part of the volcanic hydrothermal system occurs on the flanks of the volcano, with many systems drilled in order to generate geothermal power [5]. These drill holes, 1–2+ km in depth, provide information on the isotherms (flow patterns) and resulting alteration mineralogy (Fig. 1) in locations distal from the intrusive center(s). By contrast, in proximal positions drill holes are rare due to the reactive conditions and high temperature, not to mention hazards due to volcanic and hydrothermal eruption (§6.2; [6]. Information on the distribution of proximal alteration comes from exposures created by flank collapses that cause landslides and lahars (§6.1), such as on the slopes of Mt. Rainier, which reveal the alteration formed as deep as 1+ km depth [7]. Another source of information on deep alteration mineralogy and zonation comes from extinct volcanoes that host shallow-formed Au-

Ag veins, or Au-Cu deposits hosted by residual quartz and quartz-alunite alteration, once erosion removes a few to several 100s m of altered rock (Fig. 1).

The alteration closest to the discharge of high-temperature fumaroles (Fig. 1), commonly within volcanic craters (e.g., La Fossa, Vulcano, Italy) consists of a siliceous residue due to the otherwise isochemical dissolution of the rock by pH<2 solutions, with a halo of alunite and kaolin minerals (Fig. 1). On the outer margins, this grades to clay minerals, largely smectite where temperature is <150 ºC, or interstratified clays at higher temperature, and illite ± chlorite where temperature is >200–220 ºC, typically at least 200–300 m below the surface in steep terrain (Figs. 1, 4a). The residual quartz and quartz–alunite zones become wider as depth decreases, since the acid species (reaction 2) increasingly dissociate – become more reactive – at lower temperature. These patterns are well defined in Au-Cu deposits hosted by this alteration.

The hypogene acidic alteration lies over deep (1.5–2 km) biotite-K-feldspar-magnetite alteration associated with hypersaline liquid at the apex of the intrusion (Fig. 1), in the porphyry ore deposit setting [2]. These shallow and deep styles of alteration form at the same time, since vapor and hypersaline liquid are derived from the same magmatic fluid (§2; Fig. 1, deepest inclusion photograph of critical fluid exsolved from magma). The stage-2 crystallization of the intrusion exsolves magmatic liquid that, once cooled, forms a white mica-chlorite alteration overprint (Figs. 1 and 4b). The shallow thermal plume is typically offset due to the hydraulic gradient of the volcanic edifice, with outflow to the lower flanks (Fig. 1), accompanied by meteoric water dilution. The >200 ºC path is dominated by white mica alteration, with interstratified smectite clays on the lower temperature margins (Fig. 1).

3.3. Subsurface: Geophysical model

Changes in rock properties by alteration (§4.2), especially electrical resistivity derived from electrical and electromagnetic data, and magnetization derived from magnetic data, allow subsurface imaging of hydrothermal systems. Rocks that readily conduct electrical currents are dominated by connected pores and pore space contents, namely fluids as well as the high cation exchange rate due to the large surface area of clays, with typical values less than ~40 ohm-m for altered rocks saturated with groundwater, thermal fluids (mixtures of magmatic and meteoric water) (; i.e., liquid-saturated alteration, Fig. 3 top) or hypersaline liquids. In contrast, unsaturated volcanic rocks as well as residual quartz and quartz-alunite possess high electrical resistivities, typically exceeding 1000 ohm-m. Resistivity of fresh rocks is controlled by pore fluids where high saline fluids result in the lowest resistivities (<1 Ohm-m), hot geothermal fluids are moderate (~50 Ohm-m), and lower salinity and cooler groundwater are higher (~50 - 200 Ohm-m, Fig. 3 top). Porosities important for slope stability models can also be derived from resistivities of fluid saturated rocks.

Airborne electromagnetic data produce high resolution resistivity images, to as much as ~700 m depth (Fig. 3 bottom), with greater efficiency than ground-based data (below black curve, Fig. 3). Magnetization depends on grain size and volume of magnetic minerals such as magnetite and titanomagnetite, but is insensitive to the presence of fluid. Hydrothermal alteration reduces the magnetization of volcanic rocks by converting magnetite to less magnetic phases, lowering original values by a factor of three, that is, from values exceeding 3 A/m to less than 1 A/m (Fig. 3 bottom). High magnetizations (>3 A/m) are associated with fresh rocks and low values (<1 A/m) with alteration (Fig. 3 bottom).

Near-surface low resistivities (<40 ohm-m) and magnetizations (<1 A/m) (Fig. 3) correspond primarily to a combination of low temperature (<200ºC) kaolinite-alunite and smectite-Fe carbonate alteration formed in permeable layers by reactive hydrothermal fluid (§3, Figs. 1, 6c and 8d). The lowest resistivities reflect the highest clay content. These rocks are mechanically weak (§4.2) and capable of landslides (§6.1). Slope stability models that incorporate these geophysically identified regions of alteration contribute to understanding of sector/flank collapses. White mica-pyrite alteration saturated with hydrothermal liquid corresponds to moderate resistivities (~200 ohm-m) and magnetizations (~2 A/m). The deep (>1 km) low resistivities (<1 ohm-m) may correspond to ascending hydrothermal liquids (red arrow, Fig. 3) that can provide metals to potential ore deposits (§5.1, Fig. 1).

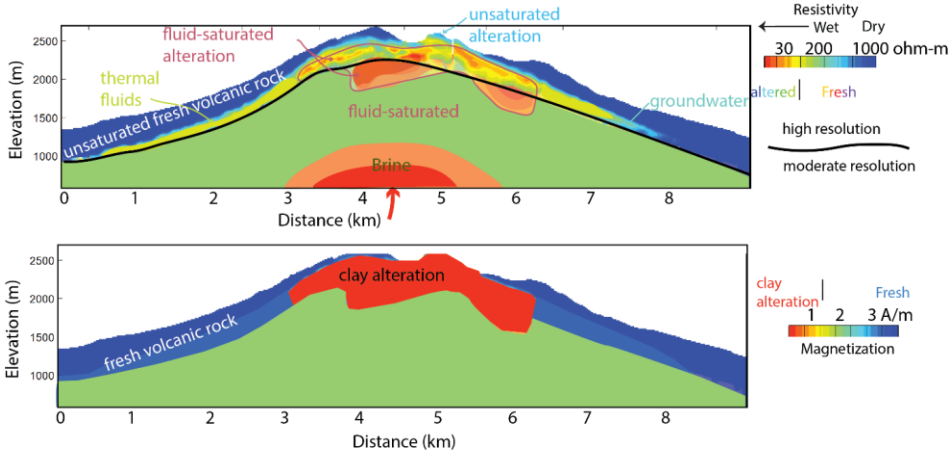

Fig. 3 Cross section from representative resistivity (top) and magnetization (bottom) models (modified from Peacock et al., 2016; Peterson et al., 2020; Miller et al., 2016 and references therein). The upper ~400 m of the resistivity model (above black line) is higher resolution than the lower portion. Both data sets discriminate fresh volcanic rocks from hydrothermally altered clays. The magnetization model is not sensitive to fluids.

4. Formation of alteration

4.1. Physico-chemical conditions

Alteration minerals formed under acidic conditions include sulfates (alunite and anhydrite), aluminosilicates (including kaolinite, halloysite, dickite, pyrophyllite, andalusite), and diaspore, associated with illite and smectite clays; many of these minerals have specific ranges of thermal stability (Fig. 4a). As noted above, these minerals form in four distinctly different environments of hydrolytic alteration, with pH range of ~1 to 4–5 (Fig. 4b). These are the hypogene setting (reactions 1+2) and steam-heated environs (reactions 3 and 4), from of 500 m+ to the surface; the fourth setting, supergene oxidation of pyrite, can form pH solutions with pH<1 (reaction 5).

Acidic solutions that alter the host rock can either weaken, or locally strengthen, the volcanic edifice stability, depending on the mineralogy (§6.1).

Acid formation in the hypogene environment (reactions 1, 2, stage 1) creates hydrothermal solutions with pH<2. This leads to a high solubility of Al and Fe hydroxides but low solubility of SiO_2, which is in solution as silicic acid, H_4SiO_4. As a result, dissolution of the host rock is close to isochemical, but with a siliceous residue left. The residual siliceous material, eventually recrystallized to quartz, commonly has a vuggy texture due to dissolution of phenocrysts. Rock dissolution neutralizes the acidic solution (orange dashed lines, Fig. 4b), such that alunite and kaolinite (or dickite or pyrophyllite at higher temperatures) become stable, forming a halo to the residual quartz (Fig. 1). The initially barren residual quartz and quartz-alunite form a horizon where a permeable lithologic unit is intersected by a feeder structure, called a lithocap. The lithocap - largely barren of metals on formation - may subsequently become mineralized if, during stage 2, white-mica–stable liquid ascends and precipitates copper and gold. In this case, the metal-bearing liquid evolves from the occurrence of chalcopyrite ($CuFeS_2$) in the porphyry deposit environment [2] to enargite (Cu_3AsS_4) or covellite (CuS) stability during cooling, due to the lack of buffering capacity of the leached rock of the lithocap.

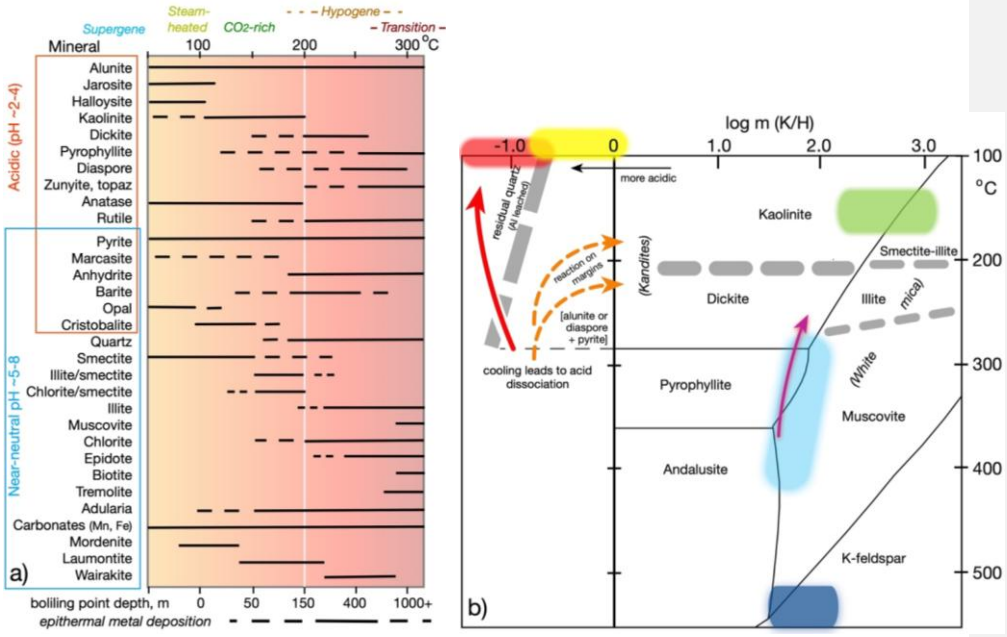

Fig. 4 a) Temperature stability of minerals, <100-300 °C and surface to ~1 km depth, the typical of range of epithermal deposit formation (modified from [8]). Boiling point depth refers to that of saturated H_2O vapor pressure at hydrostatic conditions. b) Fluid compositions and pathways for four hydrothermal alteration environments (after experimental studies by Hemley and Jones (1964); K/H=[KCl+K^+]/[HCl+H^+]). Reaction path of cooling hypogene acids (reactions 1, 2; red

arrow) enters residual quartz stability since Al-hydroxide solubility increases sharply at pH <2, resulting in dissolution of aluminosilicate minerals. Reaction with fresh rock on margins increases solution pH (orange), forming halos of alunite and kaolin. Hypogene acidic springs (red bar, pH~1–2) and steam-heated acid-sulfate springs (yellow, pH ~2-4, reaction 3), as well as CO_2-rich steam-heated solution (green, pH 4-5, >100°–150+°C, reaction 4), form clays and kaolinite. Cooling from white mica stability lead to pyrophyllite formation (purple arrow, <350°C). High-temperature porphyry alteration at 1.5-2+ km depth: stage-1 intrusion-hosted (dark blue, K-feldspar±biotite) with white mica stage-2 overprint (light blue; Fig. 1; Simon et al. this volume). Modified from [8].

Some epithermal deposits overlie deeper intrusion-hosted porphyry deposits [2]. Early feldspar-stable (stage 1) alteration of the porphyry deposit, with biotite and magnetite, is typically overprinted by white mica and chlorite (stage 2); continued ascent and cooling of the white mica–stable liquid results in pyrophyllite (± diaspore) becoming stable at <350 ^{o}C (at ~1-1.5 km depth; Fig. 4b, purple arrow). At epithermal depths, the white mica-stable liquid may deposit metals in fractures to form quartz veins with Cu, Zn and Fe sulfides (chalcopyrite, sphalerite and pyrite, respectively), plus white mica alteration (Fig. 1, light blue) on the margin of the volcanic edifice (Fig. 1, dashed pink line, i.e., older, extinct hydrothermal discharge). Steam-heated alteration of friable kaolinite and alunite typically lies over epithermal deposits, unless eroded (Fig. 1). Deeper CO_2-rich steam-heated solutions, diluent of the ascending metal-bearing NaCl liquid, form smectite, kaolinite, and Fe-Mn carbonate alteration on the margin of the system. The supergene acid source (reaction 5) can acidify groundwater to pH<1 if abundant pyrite is exposed and oxidized. This acidic solution causes ambient-temperature alteration of altered rock to kaolinite and Fe oxy-hydroxides, commonly reducing rock strength.

4.2. Formation of alteration: Physical properties

Hydrothermal alteration changes the physical, mechanical, and hydraulic properties of volcanic rocks, since it promotes (1) the replacement of primary minerals with either weak secondary minerals, such as clay minerals or alunite, or strong minerals, such as calcite or silica phases, and (2) changes in porosity (dissolution increases porosity and mineral precipitation reduces porosity). Permeability can be increased by mineral dissolution, promoting fluid flow, and decreased by void-filling precipitation (Fig. 5), promoting pore pressure build-up that can lead to increased deformation and instability (§6.1) and explosive behavior (§6.2). Strength (compressive and tensile), Young's modulus (e.g., stiffness of the rock), and cohesion can be decreased by mineral dissolution and the replacement of primary minerals with weak secondary minerals (Fig. 5), leading to an increase in instability and, potentially, mass wasting and secondary volcanic hazards (§6.1), as observed at Whakaari (New Zealand), Yellowstone (USA), La Soufrière (French Overseas Department of Guadeloupe), Ontake and Aso (Japan), Poás and Turrialba-Irazú (Costa Rica), among many others. Mineral precipitation and the replacement of primary minerals with strong secondary minerals can increase strength (compressive and tensile), Young's modulus, and cohesion (Fig. 5), and can transform unconsolidated deposits and fragmented material into coherent rock, as seen at, for example, Yellowstone's geyser basins (USA) and Ohakuri (New Zealand). The fragmentation threshold can also be increased or decreased by precipitation or dissolution, respectively (Fig. 5), thus changing the likelihood of eruptive

behavior (§6.2). Finally, alteration-induced changes to the physical, mechanical, and hydraulic properties of volcanic rocks influence the creation of geothermal and epithermal resources (§5.1).

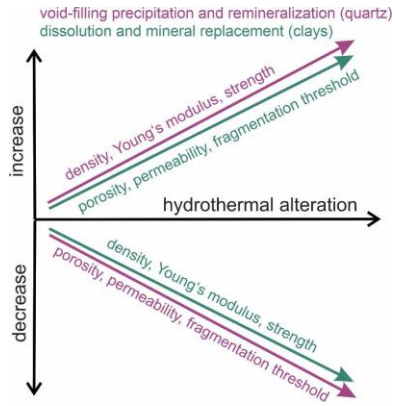

Fig. 5 Schematic diagram showing how different types of alteration can modify rock physical properties.

5. Resources

5.1. Epithermal ore deposits

Metals are commonly precipitated from hydrothermal systems near volcanic vents at shallow levels, <1 km depth, forming epithermal deposits. Many such deposits are hosted by young, partly eroded volcanoes (<1–25 Ma) around the circum Pacific, through to deeply eroded volcanoes preserved in much older belts throughout the world. There are two principal tectonic settings of formation of epithermal deposits: 1) hosted by arc volcanoes, within 1–5 km of the volcanic vent (actively forming in Japan through the Philippines to Indonesia), the setting discussed here, and 2) that associated with extension and crustal thinning, such as the gold-rich but sulfide-poor quartz veins formed in basins behind volcanic arcs (Taupo Volcanic Zone, New Zealand), or related to plumes of magma rising from the mantle (Yellowstone, USA). Examples of these types of low-salinity (<1 wt% NaCl eq.), gold-rich epithermal deposits are common in central and northern Nevada, USA. The only acidic fluids associated with these deposits are zones of steam-heated alteration (reactions 3 and 4) or post-hydrothermal weathering of pyrite (reaction 5).

Volcanic hydrothermal systems are common on calc-alkaline volcanoes in subduction-related arcs, resulting in a variety of metal deposits formed at depths of ~3–4 km up to the original surface (Fig. 1). Deposits of copper as well as gold and molybdenum, hosted by porphyrytic intrusions at a few km depth [2], account for ~70% of the global mined copper and 50% of molybdenum [3]. More shallow epithermal deposits of gold, silver and Cu±Pb-Zn plus minor critical metals (Bi, In, Sb, Se, Te) are spatially related to these intrusive centers or their margins (Fig. 1). The study of active volcanoes and their hot springs (Fig. 2) has improved the

understanding of how these metal deposits are related to their intrusion parents, and how to better explore these extinct volcanoes for their contained resources of critical metals [3].

The siliceous residue, recrystallized to quartz (Fig. 6a), has systematically zoned alteration halos (Fig. 1), from alunite (Fig. 6b), dickite or kaolinite (formed at pH~2–4), and outward to clays (illite to smectite, formed at pH~4–6; Fig. 4b). The most-altered rocks were originally the most permeable (typically welded - brittle - volcanic tuffs), whereas impermeable lava flows tend to be less altered; unwelded tuffs are typically clay altered. These leached and altered rocks form lithocaps, with one (or more) feeder zone(s), such as faults, or margins of domes, volcanic vents, or diatremes (Fig. 1). Despite the strong alteration, this stage is barren of metals, since the high-temperature vapor (up to 900 ºC) has a low metal content. However, if the subsequent stage 2 liquid, associated with white mica alteration overprint of the deeper porphyry intrusion, ascends along the feeder zone(s), copper and gold may deposit in fractures within residual quartz of the feeder zone (Fig. 6b) and lithocap (§3.1), near the volcanic vent (Fig. 1). The shallow blankets of steam-heated kaolinite (Fig. 1) may be partly (Fig. 6c) or completely eroded.

Fig. 6 a) Rhyolite atop Satsuma Iwojima, leached by acidic condensate to residual quartz, ~95 wt% SiO_2 (JWH). b) Fracture pathway of acidic liquid in volcanic dome; residual quartz (center,

~5 m wide), host for Au-Cu ore, with symmetric halo of quartz-alunite out to clays, Summitville deposit, USA (C.G. Cunningham). c) Steam-heated horizon of kaolinite, over lithocap-hosted Salares Norte epithermal gold deposit, Chile (JWH). d) Banded quartz and pink rhodochrosite vein with white mica alteration halo (dashed contact, right), Arcata epithermal Ag-Au mine, Peru. e) inset: Colloform quartz-sulfide vein of Kochbulak Au-polymetallic deposit, Uzbekistan (10 cm wide)(JWH).

Structures on the flanks of the volcanic edifice act as upflow conduits for the liquid that forms white mica alteration (the ~5–10+ wt% NaCl eq. liquid that is diluted by meteoric groundwater or CO_2-rich steam-heated solutions during ascent; Fig. 1). This cooling liquid, commonly boiling, precipitates quartz (Fig. 6d) or colloidal silica as colloform bands in veins (Fig. 6e), as well as sulfate (anhydrite, barite) and carbonate minerals (particularly Mn-rich, e.g., rhodochrosite; Fig. 6d) in fractures, along with silver and gold ± base metals (Pb as galena, Zn as sphalerite and/or Cu as chalcopyrite). These veins form marginal to the volcanic vent, up to several km distance (Fig. 1, quartz veins on eroded right margin), in contrast to proximal lithocap-hosted copper and gold deposits. In Mexico and Peru, base metal veins may have vertical intervals of ore that are 200–400 m to as much as 800 m, and are the major source of global silver.

Exploration for epithermal deposits, either hosted by residual quartz (Fig. 6a) or quartz veins (Fig. 6d, e), is guided in part by zoned alteration mineral assemblages, both in terms of reactivity (paleo-pH; Fig. 4b) as well as thermal stability (paleo-thermometers; Fig. 4a). This zonation helps geologists target the zones with highest paleo-temperature [4], i.e., where the potentially metal-bearing liquid had the highest rates of liquid upflow (pink arrows, Fig. 1).

5.2. Sulfur deposits

Elemental sulfur is formed by cooling of volcanic gases (reaction 6) or SO_2 disproportionation reaction in hydrothermal fluids (reaction 7):

$$3SO_2(aq) + 2H_2O(l) = 2H_2SO_4(aq) + S_e(s/l) \quad (7$$

Reaction 6 occurs when volcanic vapor rich in SO_2 and H_2S ascends to the surface and discharges as fumaroles at a relatively low temperature (<200 °C). Sulfur may be deposited along the vapor pathway but is more effectively produced by cooling at fumarolic vents, forming yellow sulfur deposits or a sulfur chimney (Figs. 2b and 8e). Reaction 7 involves hydrothermal liquids and is the source of strong acidity due to H_2SO_4 formation, and can occur both at deep and shallow levels, including below crater lakes. Elemental sulfur, produced in solid or liquid forms via reaction 7, may act as a sealant of the permeable vent, potentially creating conditions favorable for a hydrothermal eruption. Sulfur was previously mined from volcanoes until overtaken by sulfur production as a byproduct of oil refining, although small-scale mining continues in places like Ijen (Fig. 8f; Case Study Box) and Welirang volcanoes in Indonesia.

6. Hazards

6.1. Mass wasting (landslides and lahars)

Evidence from geological, geophysical, geochemical, and modelling studies highlights that hydrothermal alteration typically increases the instability of a volcanic structure (e.g., edifice, dome, flank, caldera). Alteration progressively changes the physical, mechanical, and hydraulic properties of the rocks that comprise a volcanic structure (§4.2); this can lead to a wide range of volcanic hazards, from small mass-wasting events such as rockfalls, to large dome, flank, or sector collapses (Fig. 7; [9]). Large collapses may also trigger other secondary hazards, such as hydrothermal eruptions (§6.2), clay-laden lahars[10], and even the formation of potentially devastating pyroclastic density currents [11]. Lahars sourced from hydrothermally altered materials, particularly with matrices of clay minerals, are transported much further down drainages than those derived from unaltered materials, and are more hazardous as a result [7].

For example, hydrothermal alteration contributed to flank collapse and subsequent lahar formation at Casita volcano, Nicaragua [12]. Persistent hydrothermal activity had weakened the edifice of Casita volcano and, as a result of Hurricane Mitch in 1998, a steep slope consisting of hydrothermally altered and brecciated lava and tephra collapsed to form a debris flow that eventually transformed into a lahar that destroyed the towns of El Porvenir and Rolando Rodríguez, killing more than 2,500 people. Large collapses thought to be promoted by hydrothermal alteration have been documented at many other volcanoes, including those of Mount Rainer (USA), Soufrière Hills volcano (Montserrat), La Soufrière de Guadeloupe (Caribbean), Turrialba-Irazú (Costa Rica), Nevado del Ruíz (Columbia), and Cayambe volcano (Ecuador).

Ongoing hydrothermal activity at many active and dormant volcanoes is progressively increases the risk of potentially devastating mass-wasting events, exacerbated by heavy rainfalls, and which are compounded by settlements locally encroaching on these slopes. Modelling indicates that an increase in the size of the hydrothermally altered zone on the southern flank of La Soufrière de Guadeloupe will increase the instability of the flank, potentially leading to collapse [13]. The increased awareness of the effect of hydrothermal alteration on volcano stability has prompted an increase in studies aimed at improving methods to monitor the extent and evolution of alteration at volcanoes with active hydrothermal systems. One important factor for volcano monitoring is the observed link between heavy rainfall, hydrothermal alteration, and volcanic instability and collapse. Dome collapses in the late 1990s and early 2000s at Soufrière Hills, Montserrat were all associated with intense rainfall in the hours prior to collapse. Instances of alteration-induced volcano instability and collapse, as well as the formation of clay-laden lahars, may increase if there is an increase in heavy rainfall, as predicted given the current trend in global climate change.

Most volcano instability and collapses associated with hydrothermal alteration are typically attributed to the formation of clay minerals and rock weakening. However, since hydrothermal alteration can either increase or decrease porosity (§4.2), it may either decrease or increase rock strength. Although increases in strength could help stabilize a volcanic structure, void-filling mineral precipitation can decrease permeability, increase pore fluid pressure, and promote volcano instability and hydrothermal eruption (§6.2). Studies to help better understand the distribution of hydrothermal alteration, alteration types, and porosity-increasing and porosity-decreasing alteration, and the timescales required for hydrothermal alteration, need to be combined with geological, geophysical, and geochemical surveys plus laboratory experiments, remote sensing, and modelling, to better predict volcanic hazards related to alteration.

6.2. Hydrothermal and phreatic eruptions

Hydrothermal and phreatic eruptions are common in volcanic hydrothermal systems [14]. These eruptions are driven by the violent expansion of H_2O liquid to vapor, which converts thermal to mechanical energy. Hydrothermal eruptions may result from expansion of hydrothermal fluid through flash boiling without direct magmatic input [15]. Hydrothermal eruptions are common, but as no magma intrusion or change in degassing is needed they often lack clear precursory signals. They are short-lived events (minutes to days) with highly variable eruption dynamics. Their associated eruption products range from large ballistic clasts to abundant fine and altered particles in energetic vapor-rich density currents to wet jets of poorly sorted rock debris. They can be very hot (>100 ºC, as pressurized steam is involved), and are accompanied by gases from the hydrothermal system (§2).

By contrast, during phreatic eruptions, magmatic heat (for instance, caused by dike intrusion) is added to cooler ground or surface water (crater lakes, hydrothermal systems), causing eruption. Despite their relatively small size, phreatic eruptions have recently caused numerous fatalities, particularly to tourists, such as in the 2014 eruption of Ontake (Japan, 63 deaths) and the 2019 Whakaari eruption (New Zealand, 22 deaths). Many conditions can lead to phreatic eruptions (§2), and numerous factors affect the diversity of eruption and related hazards [15, 16]. Key factors are (i) volume and nature of the fluid (liquid, vapor, or liquid+vapor; pH, including the abundance and relative proportions of gases such as SO_2, H_2S and CO_2), (ii) pressure and temperature evolution (absolute difference and rate of changes) from source region to surface, (iii) physical properties (porosity, permeability, strength, sealed vs open systems) of the host rocks and their changes as result of hydrothermal alteration (§4.2).

Precipitation of hydrothermal minerals such as silica polymorphs (quartz, chalcedony, opal), sulfates (alunite, jarosite, gypsum, anhydrite), elemental sulfur, or calcite can prime aquifers for eruption by sealing permeable pathways, leading to build-up of fluid pressure until it exceeds the lithostatic pressure plus tensile strength of the rock. Alternatively, alteration and rock dissolution may lead to the triggering of eruptions due to a reduced strength of the host rocks. Such weakened lithologies might also prime spots for landslides, which in turn causes a sharp pressure decrease that leads to a hydrothermal eruption (Fig. 7). Other triggers of eruptions that are being primed include seismic-induced fracturing of mineral seals, as well as the accumulation of gases due to magmatic exsolution. This chain of processes highlights that many of the hazards mentioned here, including alteration and landslides (Fig. 7), may be linked.

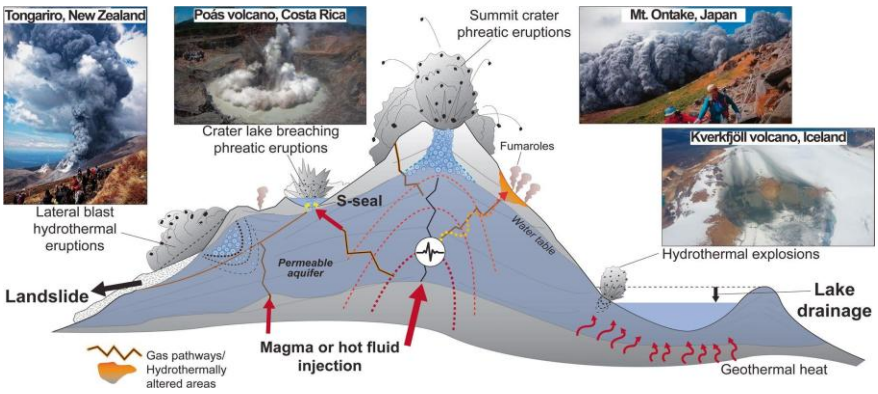

Fig. 7 Conceptual sketch of typical phreatic and hydrothermal eruption types in volcanic and hydrothermal settings, showing potential trigger mechanisms (e.g., magma/fluid injection; landslide; sudden lake drainage; or mineral sealing, e.g., by sulfur (the S-seal). Examples of eruption variations, from Te Maari-Tongariro, New Zealand (2012), Poás, Costa Rica (2014), Mt. Ontake, Japan (2014), and Kverkföll-Gengissig, Iceland (2013). From [16]. Note: vertical exaggeration of 2:1.

Commented [JH1]: Phreatic eruption term is not used in the caption, so this figure will be confusing to the reader, as 2 of the 4 photos say phreatic.

At Mt. Ontake, the eruption products were rich in altered material from the hydrothermal system! And hard to imagine that the Poas eruptions did not involve any of the hydrothermal system… (like that at White Island). Should be more rigorous than what Montanaro produced. By contrast, at Tongariro I recall that there was no evidence for hydrothermal involvement.

6.3. Acid drainage

Acidic solutions drained from volcanic crater lakes and subsurface hydrothermal reservoirs can enter watersheds, acting as a source of acidity and high concentrations of gas- and rock-derived chemical elements in surface and groundwater. Copahue (Argentina), Ijen (Indonesia) and Poás (Costa Rica) volcanoes are notable examples of acid drainage. Similarly, rivers on the flanks of active volcanoes may become acidic due to inflows from hot spring waters. For instance, the Agatsuma and Shibukuro rivers in Japan are strongly affected by acid discharges from the Kusatsu (Kusatsu-Shirane volcano) and Tamagawa (Akita–Yakeyama volcano) hot springs, respectively.

Hydrothermal acid inputs deteriorate river infrastructures, which are mainly composed of concrete and iron materials. They also pose a threat to water quality, creating both environmental and health hazards. This is due to the low pH values, increased solubility of aluminum and enhanced transport of metallic trace elements (MTE). Elevated concentrations of aluminum and MTEs render the water unsafe for domestic, agricultural, or industrial purposes. Additionally, hydrothermal solutions with a direct component of magmatic volatiles may contain high concentrations of fluoride, which affects aquatic biodiversity and higher trophic levels such as livestock and humans. Typically, there are few signs of life near the source of volcanic acid inputs. However, a gradient develops downstream as dilution occurs and solutions are neutralized by interaction with the riverbed; spatial patterns, extending from the volcano to the sea, exist in the biota and nutrient cycles of streams draining areas affected by volcanic hydrothermal activity.

Downstream processes decrease the aluminum and MTE concentrations in hydrothermally contaminated water, such as water-rock interaction, dilution with meteoric water, and sorption

onto solid phases resulting from an increase in pH plus precipitation. In Japan, crushed limestone is used to neutralize the natural acidity of the tributaries that feed into the Agatsuma river, a treatment operated for more than 50 years. However, this approach is costly and difficult to sustain. An environmental health hazard arises when river water affected by acidic solutions from a volcanic source is used for crop irrigation, potentially leading to soil acidification and increased concentrations of MTEs in soil, food and groundwater wells, thereby exposing humans to toxic levels of component. This scenario occurs in eastern Java where ~3500 ha of agricultural lands have been irrigated for several decades with river water that has a pH of 3.0–4.5, along with elevated concentrations of aluminum, MTEs and fluoride. Attempts were made in the past to minimize this impact by regulating the overflow from the Ijen crater lake, located ~30 km upstream, which was the main source of acid water. However, changes to the hydrology no longer permit this.

Case Study Box: Ijen volcano

Ijen volcano in East Java, Indonesia, is a natural observatory for many of the features described in this chapter. It is an active basaltic to dacitic stratovolcano in Ijen Caldera, with an associated volcanic hydrothermal system, i.e., a “wet" volcano. The volatiles degassed from the magma discharge at the surface from fumaroles, but also interact with the subsurface hydrothermal system to form hyperacidic solutions. Ijen’s summit hosts the largest acidic crater lake in the world, Kawah Ijen (Fig 2c), with ~27 × 10^6 m^3 of warm (>35 ˚C) mineralized solutions (pH~0, dissolved solids ~100 g/kg). The hyperacidic solutions discharge as warm springs and also seep from the crater lake to form the headwaters of the Pahit River (“bitter” river, Fig 8a), with abundant gypsum depositing at the outflow (Fig. 8b).

Stable isotopic compositions indicate that the hydrothermal solution is mainly meteoric water, with addition of magmatic volatiles. Interaction of these hyperacidic solutions with their host rocks (§4.1) leads to isochemical dissolution, as seen in altered host-rock fragments ejected during eruption. Such alteration is also occurring on the shore of the crater lake and in the Pahit riverbed (Fig. 8a), with dense, grey lavas converted to friable, whitish material (Fig. 8b, c).

Acidic alteration at Ijen dissolves fresh minerals and glass, leaving residual amorphous silica (Fig. 8c). Precipitates of pyrite and aluminum-sulfates are common (Fig. 8d), composed of alum and jarosite at the surface, and alunite in samples from deeper in the system. The fumaroles deposit elemental sulfur (Fig. 8e, §5.2), which have been mined since the 18th century (Fig. 8f), initially for gunpowder and at present for bleaching sugar. This environment is the active analog to extinct systems, where lithocaps of siliceous residue, now recrystallized to quartz, and halos of alunite-quartz-pyrite and aluminosilicates formed (Fig. 6a and b, §4.1). Such barren alteration zones may subsequently be mineralized to form epithermal Cu-Au and Ag-base metal ore deposits (§5.1).

Rock falls and slides from the steep slopes are common, likely promoted by intense alteration that reduces the strength of the rocks (§6.1). Other hazards are related to eruptions (§6.2) that may lead to lake expulsion. The last major eruption of Ijen occurred in 1817, a phreato-magmatic event that expelled lake water and produced corrosive lahars that reached Banyuwangi, the major ferry hub between Java and Bali. It devastated the cultivated areas downstream and deposited a layer of sulfur- and metal-laden mud that polluted soils and water sources.

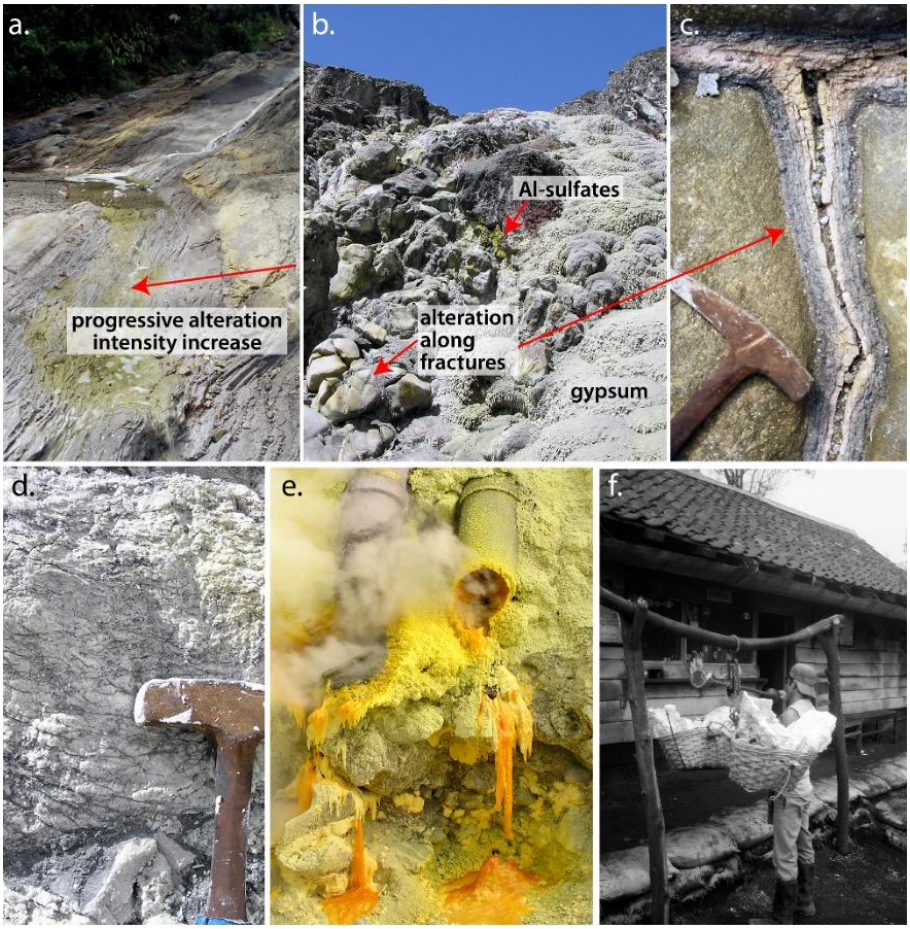

Fig. 8 a) Progressive alteration of basaltic-andesite lava in the Pahit River by pH ~1 fluids b) and c) Gypsum and Al-sulfates deposits from Ijen crater lake seepage, with alteration zonation along fluid pathways. d) Alunite-kaolinite-silica phase-pyrite alteration exposed inside Ijen crater. e) Elemental sulfur deposits (reaction 6 and 7) by cooling fumarole vapors in pipes installed for sulfur mining. f. Sulfur miner (all photos by VV).

7. Summary

Acidic solutions form where magmatic vapor condenses into groundwater at shallow depth (<100s m), resulting in the host rocks altering to sulfate and aluminosilicate minerals, mainly clays. These minerals are zoned along thermal and chemical gradients within the hydrothermal systems. The most acidic solutions (pH<2) in permeable conduits near the volcanic center leach the rock, leaving a siliceous residue, with clays formed in distal halos. These reactions affect the density, porosity, and mechanical strength of altered volcanic rocks, which may increase or decrease depending on the reactions. The resulting heterogeneous distribution of physical properties commonly leads to instabilities of the volcanic edifice or decreases in permeability, leading to mass movements or hydrothermal eruptions, respectively. Subsequent ascent of magmatic-hydrothermal liquids along the altered conduits may transport metals and form epithermal ore deposits. Acidic alteration leads to large changes in the minerals, textures, and physical properties of rocks, strongly influencing the shallow environment of volcanic edifices.

References

[1] Shinohara, H., 2013, Volatile flux from subduction zone volcanoes: Insights from a detailed evaluation of the fluxes from volcanoes in Japan: *Journal of Volcanology and Geothermal Research*, v. 268, doi:10.1016/j.jvolgeores.2013.10.007

[2] Simon, A., et al. (this volume) Formation and utilization of crustal magmatic ore deposits (porphyries, skarns and pegmatites).

[3] Sillitoe, R.H., 2010, Porphyry copper systems: *Economic Geology*, v. 105, p. 3–41.

[4] Giggenbach, W.F., 1996, Chemical composition of volcanic gases, *in* Scarpa, R., and Tilling, R.I., eds., Monitoring and mitigation of volcanic hazards: Berlin, Springer-Verlag, p. 221–256.

[5] Scott, S., et al. (this volume) Mining heat from geothermal systems in volcanic terrain

[6] Lavallee, Y., et al. (this volume) Exploring and exploiting the magma-hydrothermal interface and super-critical systems for heat and metals

[7] John, D.A., Sisson, T.W., Breit G.N., Rye, R.O., and Vallance, JK.W., 2008, Characteristics, extent and origin of hydrothermal alteration at Mount Rainier Volcano, Cascades Arc, USA: Implications for debris-flow hazards and mineral deposits: *Journal of Volcanology and Geothermal Research*, v. 175, p. 289-314.

[8] Hedenquist, J.W., and Arribas, A., 2022, Exploration implications of multiple formation environments of advanced argillic minerals: *Economic Geology*, v. 117, p. 609–643.

[9] Capra, L., et al. (this volume) Volcano flank instabilities and collapse, Slope Failures.

[10] Phillips, J., et al. (this volume) Lahars

[11] Charbonnier, S. (this volume) PDCs.

[12] Opfergelt, S., Delmelle, P., Boivin, P., and Delvaux, B., 2006, The 1998 debris avalanche at Casita volcano, Nicaragua: investigation of the role of hydrothermal smectite in promoting slope instability: *Geophysical Research Letters*, v. 33, doi:10.1029/2006GL026661.

[13] Heap, M.J., Baumann, T.S., Rosas-Carbajal, M., Komorowski, J.C., Gilg, H.A., Villeneuve, M., Moretti, R., Baud, P., Carbillet, L., Harnett, C., and Reuschlé, T., 2021, Alteration-induced volcano instability at La Soufrière de Guadeloupe (Eastern Caribbean): *Journal of Geophysical Research, Solid Earth*, v. 126, doi:10.1029/2021JB022514.

[14] White, J., et al. (this volume) Eruptive Styles: Hydrovolcanic eruptions.

[15] Browne, P.R.L., and Lawless, J.V., 2001, Characteristics of hydrothermal eruptions, with examples from New Zealand and elsewhere: *Earth Science Review,* v. 52, p.299–331. https://doi.org/10.1016/S0012-8252(00)00030-1

[16] Montanaro, C., Mick, E., Salas-Navarro, J., Caudron, C., Cronin, S. J., de Moor, J. M., Scheu, B., Stix, J., and Strehlow, K., 2022, Phreatic and hydrothermal eruptions: from overlooked to looking over. *Bulletin of Volcanology*, v. 84, doi:10.1007/s00445-022-01571-7

Further readings

Delmelle, P. and Bernard, A., 2015, The Remarkable Chemistry of Sulfur in Hyper-Acid Crater Lakes: A Scientific Tribute to Bokuichiro Takano and Minoru Kusakabe: *in* Rouwet, D., Christenson, B., Tassi, F., and Vandemeulebrouck, J., eds., *Volcanic Lakes*: Springer Berlin Heidelberg: p. 239-259.

de Moor, J. M., Stix, J., Avard, G., Muller, C., Corrales, E., Diaz, A., Alan, A., Brenes, J., Aiuppa, A. and Fischer, T. P., 2019, Insights on Hydrothermal Magmatic Interactions and Eruptive Processes at Poás Volcano (Costa Rica) From High-Frequency Gas Monitoring and Drone Measurements. *Geophys Research Letter*., v. 46, p.1293–1302. https://doi.org/10.1029/2018GL080301

Giggenbach, W. F., 1987, Redox processes governing the chemistry of fumarolic gas discharges from White Island, New Zealand: *Applied Geochemistry*, v. 2, 143-161.

Heap, M. J., Baumann, T., Gilg, H. A., Kolzenburg, S., Ryan, A. G., Villeneuve, M., Russell. J.K., Kennedy, L.A., Rosas-Carbajal, M. and Clynne, M. A., 2021, Hydrothermal alteration can result in pore pressurization and volcano instability: *Geology*, v. 49, p. 1348-1352.

Heap, M. J., Troll, V. R., Kushnir, A. R., Gilg, H. A., Collinson, A. S., Deegan, F. M., Darmawan, H., Seraphine, N., Neuberg, J. and Walter, T. R., 2019, Hydrothermal alteration of andesitic lava domes can lead to explosive volcanic behaviour: *Nature Communications*, v.10, doi:10.1038/s41467-019-13102-8.

Heap, M. J., Gravley, D. M., Kennedy, B. M., Gilg, H. A., Bertolett, E., and Barker, S. L., 2020, Quantifying the role of hydrothermal alteration in creating geothermal and epithermal mineral resources: The Ohakuri ignimbrite (Taupō Volcanic Zone, New Zealand): *Journal of Volcanology and Geothermal Research*, v. 390, doi:10.1016/j.jvolgeores.2019.106703.

Hedenquist, J.W., and Taran, Y.A., 2013, Modeling the formation of advanced argillic lithocaps: Volcanic vapor condensation above porphyry intrusions: *Economic Geology*, v. 108, p. 1523–1540.

Mannen, K., Tanada, T., Jomori, A., Akatsuka, T., Kikugawa, G., Fukazawa, Y., Yamashita, H. and Fujimoto K., 2019, Source constraints for the 2015 phreatic eruption of Hakone volcano, Japan, based on geological analysis and resistivity structure. Earth, Planets and Space, v. 71, doi:10.1186/s40623-019-1116-5.

Montanaro, C., Mayer, K., Isaia, R., Gresse, M., Scheu, B., Yilmaz, T.I., Vandemeulebrouck, J., Ricci, T. and Dingwell, D.B., 2017, Hydrothermal activity and subsoil complexity: implication for degassing processes at Solfatara crater, Campi Flegrei caldera, *Bulletin of Volcanology*, v. 79, doi:10.1007/s00445-017-1167.

Montanaro, C., Cronin, S. J., Scheu, B., Kennedy, B., Scott, B. J. and Dingwell, D.B., 2021, Host Rock Variability Powers the Diversity of Steam-Driven Eruptions. *Geophysical Research Letters*, v48, doi:10.1029/2020GL089025.

Morgan, L. A., Shanks, W. C. P. and Pierce, K. L., 2009, Hydrothermal processes above the Yellowstone magma chamber: large hydrothermal systems and large hydrothermal

explosions. *Geological Society of America Special Paper*, v. 459, p. 1–95. doi:10.1130/2009.2459(01).
Pola, A., Crosta, G., Fusi, N., Barberini, V. and Norini, G., 2012, Influence of alteration on physical properties of volcanic rocks: *Tectonophysics,* v. 566, p. 67-86.
Reid, M. E., Sisson, T. W. and Brien, D. L., 2001, Volcano collapse promoted by hydrothermal alteration and edifice shape, Mount Rainier, Washington: *Geology*, v. 29, p. 779-782.
Reid, M. E. 2004, Massive collapse of volcano edifices triggered by hydrothermal pressurization: *Geology*, v. 32, v. 373-376.
Rowland, J.V., and Simmons, S.F. (2012) Hydrologic, magmatic, and tectonic controls on hydrothermal flow, Taupo Volcanic Zone, New Zealand: implications for the formation of epithermal vein deposits. *Economic Geology*, v.107, p.427–457. doi:10.2113/econgeo.107.3.427
Shinohara, H., and Hedenquist, J. W., 1997, Constraints on magma degassing beneath the Far Southeast porphyry Cu-Au deposit, Philippines: *Journal of Petrology*, 38, https://doi.org/10.1093/petroj/38.12.1741
van Rotterdam-Los, A.M.D., Heikens, A., Vriend, S.P., van Bergen. M.J., and van Gaans, P.F.M., 2008, Impact of acid effluent from Kawah Ijen crater lake on irrigated agricultural soils: Soil chemical processes and plant uptake: *Journal of Volcanology and Geothermal Research,* v. 178, p. 287-296.
van Wyk de Vries, B., Kerle, N., and Petley, D., 2000., Sector collapse forming at Casita volcano, Nicaragua: *Geology*, v. 28, p. 167-170.

References for figures

Fig. 3
Miller, C.A. and Williams-Jones, G., 2016. Internal structure and volcanic hazard potential of Mt Tongariro, New Zealand, from 3D gravity and magnetic models. *Journal of Volcanology and Geothermal Research*, *319*, pp.12-28.
Peacock, J. R., Mangan, M. T., McPhee, D., and Wannamaker, P. E., 2016, Three-dimensional electrical resistivity model of the hydrothermal system in Long Valley Caldera, California, from magnetotellurics: *Geophysical Research Letters*, v. 43, p. 7953-7962.
Peterson, D. E., Finn, C. A., and Bedrosian, P. A., 2021, Airborne geophysical imaging of weak zones on Iliamna Volcano, Alaska: Implications for slope stability: *Journal of Geophysical Research: Solid Earth*, v. 126, doi:10.1029/2020JB020807.
Fig. 4
Hemley, J.J., and Jones, W.R., 1964, Chemical aspects of hydrothermal alteration with emphasis on hydrogen metasomatism: Economic Geology, v. 59, p. 538-569.